PCCP

A Combined Experimental and Computational Study on the Reaction Dynamics of the 1-Propynyl Radical (CH_3CC; X^2A_1) with Ethylene (H_2CCH_2; X^1A_{1g}) and the Formation of 1-Penten-3-yne ($CH_2CHCCCH_3$; X^1A')

Journal:	*Physical Chemistry Chemical Physics*
Manuscript ID	CP-ART-07-2019-004073.R1
Article Type:	Paper
Date Submitted by the Author:	23-Sep-2019
Complete List of Authors:	He, Chao; University of Hawai'i at Manoa, Department of Chemistry Zhao, Long; University of Hawaii at Manoa, Department of Chemistry Thomas, Aaron; University of Hawaii, Chemistry Galimova, Galiya; Samara National Research University S P Korolev Mebel, Alexander; Florida International University, Chemistry and Biochemistry Kaiser, Ralf; University of Hawaii,

A Combined Experimental and Computational Study on the Reaction Dynamics of the 1-Propynyl Radical (CH_3CC; X^2A_1) with Ethylene (H_2CCH_2; X^1A_{1g}) and the Formation of 1-Penten-3-yne ($CH_2CHCCCH_3$; X^1A')

Chao He,[a] Long Zhao,[a] Aaron M. Thomas,[a] Galiya R. Galimova,[b,c] Alexander M. Mebel,[b,c,*] Ralf I. Kaiser,[a,*]

[a] *Department of Chemistry, University of Hawai'i at Manoa, Honolulu, Hawaii 96822, USA*

[b] *Department of Chemistry and Biochemistry, Florida International University, Miami, Florida 33199, USA*

[c] *Samara National Research University, Samara 443086*

PCCP
(submitted July 2019)

* Corresponding Authors:
Prof. Ralf I. Kaiser: ralfk@hawaii.edu
Prof. Alexander M. Mebel: mebela@fiu.edu

Abstract

The crossed molecular beam reactions of the 1-propynyl radical (CH_3CC; X^2A_1) with ethylene (H_2CCH_2; X^1A_{1g}) and ethylene-d_4 (D_2CCD_2; X^1A_{1g}) were performed at collision energies of 31 kJ mol^{-1} under single collision conditions. Combining our laboratory data with ab initio electronic structure and statistical Rice-Ramsperger-Kassel-Marcus (RRKM) calculations, we reveal that the reaction is initiated by the barrierless addition of the 1-propynyl radical to the π-electron density of the unsaturated hydrocarbon of ethylene leading to a doublet C_5H_7 intermediate(s) with a life time(s) longer than the rotation period(s). The reaction eventually produces 1-penten-3-yne (**p1**) plus hydrogen atom with an overall reaction exoergicity of 111 ± 16 kJ mol^{-1}. About 35% of **p1** originates from the initial collision complex followed by C–H bond rupture via a tight exit transition state located 22 kJ mol^{-1} above the separated products. The collision complex (**i1**) can also undergo a [1,2] hydrogen atom shift to the $CH_3CHCCCH_3$ intermediate (**i2**) prior to a hydrogen atom release; RRKM calculations suggest that this pathway contributes to about 65% of **p1**. In higher density environments such as in combustion flames and circumstellar envelopes of carbon stars close to the central star, 1-penten-3-yne (**p1**) may eventually form the cyclopentadienyl (c-C_5H_5) radical via hydrogen atom induced isomerization as an important pathway to form precursors to polycyclic aromatic hydrocarbons (PAHs) and to carbonaceous nanoparticles.

1. Introduction

During the last decades, the untangling of the formation mechanisms of polycyclic aromatic hydrocarbons, (PAHs) - organic molecules carrying fused benzene rings - has received considerable attention from the physical (organic), astrochemistry, and theoretical chemistry communities due to their importance in combustion chemistry and astrochemistry. [1-12] In deep space, spectroscopic signatures of PAH-like species such as alkylated, ionized, (de)hydrogenated and protonated counterparts [13-18] have been observed in the ultraviolet (200-400 nm) and the infrared (3-20 μm) regions through the diffuse interstellar bands (DIBs) and unidentified infrared (UIRs) bands.[2-4, 19-25] With up to 20 % of the galactic carbon budget suggested to be locked in PAH-like molecules,[26] PAHs and their derivatives are potential key intermediates and nucleation sites leading eventually to carbonaceous nanoparticles ("interstellar grains").[4, 23-25, 27-29] On Earth, largely produced in the incomplete combustion of fossil fuel, PAHs are considered as critical precursors to unwanted soot particles[5] leading to combustion inefficiency and causing air pollution along with detrimental health effects culminating in cancer.[6-8] Thus, the understanding the key processes in the synthesis of PAHs along with their precursors in combustion systems and in interstellar and circumstellar environments will provide critical insights into how complex aromatic structures and possibly graphenes and fullerenes are formed.[30-51]

On the basis of the kinetic models and electronic structure calculations, the hydrogen abstraction-acetylene addition (HACA)[52, 53] mechanism has been proposed to be central in the formation of PAHs under high temperature conditions.[53-56] This mechanism implicates repetitive sequences of atomic hydrogen abstraction from the aromatic hydrocarbon followed by the subsequent addition of acetylene molecule(s) before cyclization and aromatization.[1, 3, 57, 58] Naphthalene ($C_{10}H_8$), the simplest PAH molecule which comprised of two fused benzene rings, can be produced by the phenyl radical reacting with two acetylene molecules via HACA.[53, 56, 59] HACA has been experimentally evidenced in also leading from biphenyl ($C_{12}H_{10}$) by hydrogen abstraction and subsequent addition of a single acetylene molecule to phenanthrene ($C_{14}H_{10}$).[55] Very recently, PAHs containing four rings such as pyrene ($C_{16}H_{10}$) were formed through an acetylene triggered bay-closure involving HACA.[60]

Alternatively, PAHs can be synthesized via the hydrogen abstraction – vinylacetylene addition (HAVA)[59, 61-63] pathway, which operates at low temperature due to the absence of any

entrance barrier to reaction.[64, 65] Naphthalene ($C_{10}H_8$), phenanthrene/anthracene ($C_{14}H_{10}$) and triphenylene ($C_{18}H_{12}$) are formed via reactions of phenyl (C_6H_5), naphthyl ($C_{10}H_7$), and phenanthrenyl ($C_{14}H_9$) radicals with vinylacetylene (C_4H_4), respectively, via barrier-less reactions at temperature as low as 10 K thus providing an unconventional route how PAHs may originate in cold molecular clouds and even in hydrocarbon-rich atmospheres of planets and their moons such as Saturn's satellite Titan.[63, 66, 67]

Additionally, odd-carbon radicals tend to be resonantly stabilized (RSFRs) and have been proposed to drive PAH formation under combustion conditions.[68, 69] Through experimental and kinetic modeling studies, Marinov et al. proposed that the origin of naphthalene ($C_{10}H_8$) might be resonance-stabilized cyclopentadienyl radicals (c-C_5H_5) in hydrocarbon flames.[70-72] The authors suggested – without providing evidence in terms of reactions under single collision conditions - that naphthalene can be formed by the self-recombination of cyclopentadienyl radicals, followed by hydrogen atom shifts and two hydrogen-atom ejections. Senkan et al. used the quantum chemical BAC-MP4 and BAC-MP2 methods to identify the reaction pathway to form naphthalene from two cyclopentadienyl radicals.[73] Mebel et al. proposed that at temperatures of 1,000 – 2,000 K relevant to combustion, indene molecules (C_9H_8) formed via cyclopentadienyl radical (c-C_5H_5) reactions, which is itself formed by hydrogen abstraction from cyclopentadiene (c-C_5H_6) represent the major reaction product.[74] Nevertheless, the origin of cyclopentadiene along with its structural isomers has remained elusive (Scheme 1). These isomers can be arranged in three classes: (1) cyclic molecules with a three-membered ring (A, D), (2) acyclic molecules (C, E to I, K), and (3) monocyclic isomers with a four-membered ring (B, J) and a five-membered ring (L). According to a recent photoionization mass spectrometry study coupled with electronic structure calculations, the most stable isomer cyclopentadiene (L) was found to be the prevailing C_5 species in various fuel-rich flames (1,2-propadiene, propyne, cyclopentene and benzene) exhibiting significantly higher yields compared to the acyclic C_5H_6 isomers (E to G, I, K).[75] Contributions from the (Z)-pent-3-en-1-yne (I) and 1-penten-3-yne (K) were observed, too, whereas the second most stable cyclic isomer 3-methylenecyclobut-1-ene (J) was ruled out in rich flames fueled by allene, propyne, cyclopentene or benzene.[75] Contributions from less stable isomers were difficult to identify both in combustion systems and in the interstellar medium.[75, 76]

Experimental and theoretical studies reveal that C_5H_X (x = 5, 6, 7) isomers can be formed involving bimolecular reactions of the ethynyl radical (C_2H) with propene (C_3H_6) (1),[77] carbon atoms (C) with the C_4H_6 isomers 1,3-butadiene, 1,2-butadiene, and dimethylacetylene (2-4),[78-80] and singlet/triplet dicarbon (C_2) with propene (C_3H_6) (5).[81] Li and co-workers explored the C_5H_7 potential energy surface (PES) exploiting quantum chemical calculations combined with canonical transition state theory and Rice-Ramsperger-Kassel-Marcus/master equation (RRKM/ME) theory.[77] The C_5H_6 PES was computed using the hybrid density functional B3LYP method and higher levels of theory.[78-80] 2-methylbut-1-en-3-yne (F) and atomic hydrogen were predicted as the major products in the reaction (1) involving the ethynyl (C_2H) addition to propylene (C_3H_6). Pent-3-en-1-yne (G) plus hydrogen and 4-penten-1-yne plus hydrogen are minor products from the terminal C_2H addition, which is favored at high temperatures.[77] Further, products of the gross formula C_5H_5 were formed in the reaction of ground state carbon atoms, $C(^3P_j)$, with C_4H_6 isomers, 1,3-butadiene (2),[78] dimethylacetylene (3),[79] 1,2-butadiene (4).[80] Experimental studies combined with ab initio/RRKM calculations showed that the first reaction (2) yields predominantly 1- and 3-vinylpropargyl radicals ($HCCCHC_2H_3$, $H_2CCCC_2H_3$),[78] while the second reaction (3) leads predominantly to the 1-methylbutatrienyl radical ($H_2CCCCCH_3$).[79] 3-Vinylpropargyl ($H_2CCCC_2H_3$) along with 1- and 4-methylbutatrienyl (CH_3CCCCH_2, $HCCCCH(CH_3)$) radicals were the dominant products of the third reaction (4).[80] The dicarbon plus propylene reaction (5) is initiated by the addition of the dicarbon reactant to the carbon−carbon double bond of propene.[81] At least two distinct C_5H_5 isomers were identified, i.e., the resonantly stabilized free radicals 1-vinyl-propargyl ($HCCCHC_2H_3$) and 3-vinylpropargyl ($H_2CCCC_2H_3$) formed via atomic hydrogen elimination from the former methyl and vinyl groups, respectively. In combustion flames and circumstellar envelopes of carbon stars, C_5H_X (x = 5, 6, 7) species might isomerize via a hydrogen assisted rearrangement to the thermodynamically most stable cyclopentadienyl radical, which is considered as a crucial PAH precursor.[74, 75, 82-86]

$$C_2H + CH_3CHCH_2 \rightarrow C_5H_7 \rightarrow C_5H_6 + H \quad (1)$$

$$C + H_2CCHCHCH_2 \rightarrow C_5H_6 \rightarrow C_5H_5 + H \quad (2)$$

$$C + H_3CCCCH_3 \rightarrow C_5H_6 \rightarrow C_5H_5 + H \quad (3)$$

$$C + H_2CCCH(CH_3) \rightarrow C_5H_6 \rightarrow C_5H_5 + H \quad (4)$$

$$C_2 + CH_3CHCH_2 \rightarrow C_5H_6 \rightarrow C_5H_5 + H \quad (5)$$

The aforementioned compilation reveals that the formation mechanisms of C_5H_X (x = 5, 6, 7) isomers are very complex and still far from being resolved. Here we access the C_5H_6 and C_5H_7 potential energy surface (PESs) via the barrier-less reaction of the 1-propynyl (CH_3CC) radical with ethylene (H_2CCH_2). By combining the crossed molecular beam experimental results with electronic structure calculations, we demonstrate that the 1-penten-3-yne molecule ($CH_2CHCCCH_3$, X^1A') is formed via a barrierless, single collision event involving the reaction of 1-propynyl radical with ethylene. In high-density environments such as combustion flames and circumstellar envelopes of carbon stars, these isomers might undergo hydrogen-assisted isomerization to the cyclopentadienyl radical – a potential key precursor involved in the production of PAHs and soot.[87-89]

2. Experimental and computational methods

2.1. Experimental methods

The bimolecular reactions of 1-propynyl (CH_3CC; X^2A_1) with ethylene (H_2CCH_2; X^1A_{1g}) and ethylene-d_4 (D_2CCD_2; X^1A_{1g}) were studied under single collision conditions exploiting a universal crossed molecular beams machine at the University of Hawaii.[90] The pulsed 1-propynyl molecular beam was produced by photodissociation (193 nm, 30 Hz, 20 mJ pulse^{-1}) [91] of 1-bromopropyne (CH_3CCBr; 1717 CheMall, 95 %) seeded at a level of 0.5 % in helium (99.9999 %; AirGas). The beam was introduced into a piezoelectric pulsed valve operating at 60 Hz, then skimmed and velocity selected by a four-slot chopper wheel rotating at 120 Hz, resulting in a peak velocity v_p of 1740 ± 8 m s^{-1} and speed ratio S of 8.1 ± 0.3 (Table 1). These supersonic radicals crossed perpendicularly with a pure ethylene (C_2H_4; 99.999%, AGT) gas, which was regulated at 550 Torr and also operated at 60 Hz. The ethylene velocity distribution was determined to be v_p = 890 ± 15 m s^{-1} with S = 15.7 ± 0.2 (Table 1) resulting in a nominal collision energy E_C of 31.1 ± 0.4 kJ mol^{-1} and a center-of-mass angle Θ_{CM} of 20.3 ± 0.3°. The ethylene-d_4 beam was characterized by v_p = 880 ± 15 m s^{-1} and S = 15.7 ± 0.2, which corresponds to E_C = 33.4 ± 0.4 kJ mol^{-1} and Θ_{CM} = 22.8 ± 0.3° (Table 1). The neutral products formed in the reactive scattering process were ionized at 80 eV in the detector,[92] filtered according to mass-to-charge (*m/z*) ratios using the QMS (Extrel; QC 150) equipped with a 2.1 MHz oscillator and then recorded by a Daly-type ion counter.[93]

Time-of-flight (TOF) spectra were recorded at laboratory angles between $0° \leq \Theta \leq 69°$ with respect to the 1-propynyl radical beam ($\Theta = 0°$) and integrated to obtain the product angular distribution in the laboratory frame (LAB). To extract the information about the reaction dynamics we used a forward-convolution method to transform the LAB data into the center-of-mass frame (CM).[46, 49, 94, 95] This represents an iterative method whereby user defined CM translational energy $P(E_T)$ and angular $T(\theta)$ flux distributions are varied until a best fit of the laboratory TOF spectra and angular distributions are achieved. The CM functions comprise the reactive differential cross section $I(\theta,u) \sim P(u) \times T(\theta)$ with u defined as the center-of-mass velocity. The differential cross section is plotted as a flux contour map that serves as an image of the reaction. Errors of the $P(E_T)$ and $T(\theta)$ functions are determined within 1σ error limits of the accompanying LAB angular distribution, velocities, and speed ratios of the beams.

We want to clarify here that the most stable of C_3H_3 isomer – propargyl (CH_2CCH) – might be produced as a byproduct in the preparation of 1-propynyl radical. 1-Propynyl (CH_3CC) can isomerize to propargyl (H_2CCCH) via hydrogen atom migration. However, the entrance barrier for the propargyl radical reaction with ethylene ranges between 43 and 44 kJ mol^{-1},[96, 97] which is much higher than the collision energy in our experiment of 31 kJ mol^{-1}. Therefore, we can conclude that propargyl radical reactions with ethylene do not occur under our experimental conditions and hence do not contribute to any reactive scattering signal of the title reaction.

2.2. Computational methods

Geometries of the reactants, intermediates, transition states, and products on the C_5H_7 PES were optimized at the density functional B3LYP/6-311G(d,p) level of theory.[98, 99] Calculations of vibrational frequencies were performed at the same theoretical level to evaluate zero-point vibrational energy corrections (ZPE). More accurate single-point energies were obtained using the explicitly-correlated coupled clusters CCSD(T)-F12 method[100, 101] with Dunning's correlation-consistent cc-pVTZ-f12 basis set.[102, 103] Relative energies computed at the CCSD(T)-F12/cc-pVTZ-f12//B3LYP/6-311G(d,p) + ZPE(B3LYP/6-311G(d,p)) level are expected to be accurate within 4 kJ mol^{-1} or better.[104] The GAUSSIAN 09[105] and MOLPRO 2010[103] program packages were employed for the ab initio calculations. Rice-Ramsperger-

Kassel-Marcus (RRKM) theory,[106-108] was used to compute energy-dependent rate constants of all unimolecular reaction steps on the C_5H_7 PES after the initial association of the 1-propynyl radical with ethylene. Rate constants were evaluated as functions of available internal energy of each intermediate or transition state within the harmonic approximation using B3LYP/6-311G(d,p) computed frequencies and employing our in-house code,[109] which automatically processes GAUSSIAN 09 log files to evaluate numbers of states for transition states and densities of states for local minima using the direct count method. The internal energy was taken to be equal to the sum of the collision energy and the chemical activation energy, that is, negative of the relative energy of a species with respect to the reactants. Only one energy level was considered throughout as at a zero-pressure limit corresponding to crossed molecular beam conditions. RRKM rate constants were then utilized to compute product branching ratios by solving first-order kinetic equations within steady-state approximation.[109, 110]

3. Results

3.1. Laboratory frame

Reactive scattering signal for the reaction of the 1-propynyl radical (CH_3CC; 39 amu) with ethylene (H_2CCH_2; 28 amu) was observed at mass to charge ratios (*m/z)* of 67 ($^{13}CC_4H_6^+$), 66 ($C_5H_6^+$), and 65 ($C_5H_5^+$) with signal at m/z = 65 collected at a level of about 50 % with respect to m/z = 66. The time-of-flight (TOF) spectra recorded at these mass-to-charge ratios were superimposable after scaling suggesting that signals at m/z = 66 and 65 originate from the same reaction channel forming the heavy product (C_5H_6; 66 amu) along with atomic hydrogen (H; 1 amu); signal at m/z = 65 can be attributed to dissociative electron impact ionization of the C_5H_6 product in the electron impact ionizer, whereas ion counts at m/z = 67 can be connected to the ^{13}C substituted C_5H_6 product arising from the natural distribution of carbon atom isotopes. The TOF spectra of the C_5H_6 reaction product were collected at m/z = 66 at distinct laboratory angles from 10.25° to 35.25° in 2.5° intervals with up to 1.6×10^6 TOFs per angle (Figure 1b). The resulting TOFs were then normalized with respect to the center-of-mass angle to obtain the laboratory angular distribution (Figure 1a). The laboratory angular distribution spans nearly 25° within the scattering plane and is essentially symmetric around Θ_{CM}. This result suggests most likely indirect scattering dynamics via C_5H_7 reaction intermediate(s) that dissociate to C_5H_6 plus atomic hydrogen.[111]

In order to elucidate the detailed position(s) of the atomic hydrogen loss(es), the reaction of the 1-propynyl radical (CH_3CC; 39 amu) with deuterated ethylene (D_2CCD_2; 32 amu) was performed as well. Isotopic substitution experiments are a convenient tool to extract the hydrogen atom loss position(s).[11, 12, 47, 50, 112-114] First, these studies focused on the hydrogen vs deuterium atom loss channels of 1-propynyl radical (CH_3CC; 39 amu) with ethylene-d_4 (D_2CCD_2; 32 amu). For the 1-propynyl radical (CH_3CC; 39 amu) - ethylene-d_4 (D_2CCD_2) system (reactions (6)-(7)), TOFs were recorded at *m/z* = 70 ($C_5H_2D_4^+$) (6) and *m/z* = 69 ($C_5H_3D_3^+$) (7) at the CM angle of 22.8°; strong signal was observed at m/z = 69 (Figure 2). A very weak signal was observed at *m/z* = 70, which can account for the ^{13}C signature of m/z = 69. Consequently, signal at *m/z* = 69 is attributed to the formation of $C_5H_3D_3$ resulting from an exclusive *deuterium atom loss* channel from the deuterated ethylene reactant. Therefore, no atomic hydrogen was emitted from the methyl moiety of the 1-propynyl radical (CH_3CC) within our detection limits. In summary, the isotopic experiments reveal that for the 1-propynyl (CH_3CC) – ethylene (H_2CCH_2) system, the hydrogen loss originates solely from ethylene.

$$H_3CCC\ (39\ amu) + D_2CCD_2\ (32\ amu) \rightarrow C_5H_2D_4\ (70\ amu) + H\ (1\ amu) \quad (6)$$

$$H_3CCC\ (39\ amu) + D_2CCD_2\ (32\ amu) \rightarrow C_5H_3D_3\ (69\ amu) + D\ (2\ amu) \quad (7)$$

3.2. Center-of-mass frame

For the 1-propynyl radical (CH_3CC; 39 amu) with ethylene (H_2CCH_2; 28 amu) reaction, the TOF spectra and LAB angular distribution can be fit with a single reaction channel with the products of the generic formula C_5H_6 and atomic hydrogen. The best-fitting CM functions are shown in Figure 3 with the hatched areas of the $P(E_T)$ and $T(\theta)$ determined within the 1σ error limits of the LAB angular distribution. The maximum energy E_{max} of the center-of-mass translational energy distribution $P(E_T)$ (Figure 3) is represented by $E_{max} = E_C - \Delta_r G$ for those molecules born without internal excitation. E_{max} was derived from the $P(E_T)$ as 142 ± 16 kJ mol^{-1} which suggests a reaction exoergicity of 111 ± 16 kJ mol^{-1} to form C_5H_6 plus atomic hydrogen. The distribution maximum at 27 kJ mol^{-1} indicates a tight exit transition state leading to C_5H_6 from the C_5H_7 intermediate(s). An average translational energy of 50 ± 6 kJ mol^{-1} suggests that 35% of the energy is channeled into product translation suggesting indirect scattering dynamics. Finally, additional information on the reaction dynamics can be obtained by inspecting the CM angular distribution, $T(\theta)$ (Figure 3b). $T(\theta)$ displays forward-backward symmetry and non-zero

intensity from 0 to 180° suggesting that the lifetime of the intermediate C_5H_7 is longer than its rotational period(s).[111] The maximum at 90° in the *T(θ)* distribution highlights geometrical constraints on the decomposing complex ("sideways scattering") revealing that the hydrogen atom is eliminated preferentially perpendicularly to the plane of the decomposing complex and almost parallel to the total angular momentum vector.[111, 115]

4. Discussion

Here we combine our experimental data on the dynamics leading to C_5H_6 formation with electronic structure and statistical calculations to reveal the underlying reaction mechanism(s) (Figures 4-7, Table 2). The doublet C_5H_7 potential energy surface was developed connecting the 1-propynyl radical plus ethylene entrance channel via eight C_5H_7 intermediates and seventeen transition states to atomic hydrogen loss C_5H_6 products **p1-p7** (Figure 4). The 1-penten-3-yne (**p1**, C_1), penta-1,2,3-triene (**p2**, C_s), penta-1,2,4-triene (**p3**, C_s), 3-methylenecyclobut-1-ene (**p4**, C_s), cyclopentadiene (**p5**, C_{2v}), penta-1,2,4-triene (**p6**, C_s) and vinylidenecyclopropane (**p7**, C_{2v}) isomers can be formed along with the light hydrogen atom with computed reaction energies of -112, -69, -105, -109, -224, -96, and -27 kJ mol^{-1}, respectively, with error bars of 4 kJ mol^{-1}. The computed reaction energy for the formation of 1-penten-3-yne (**p1**), penta-1,2,4-triene (**p3**), 3-methylenecyclobut-1-ene (**p4**), and penta-1,2,4-triene (**p6**) plus atomic hydrogen of -112, -105, -109, and -96 kJ mol^{-1} correlate within the error limits with our experimentally derived reaction energy of −111 ± 16 kJ mol^{-1}. Regarding the high-energy **p2** and **p7** isomers, a comparison of the experimental and computed reaction energetics is insufficient to exclude their formation, since they might be masked in the low energy section of the center-of-mass translational energy distribution. If solely formed, the translational energy distributions for **p2** and **p7** would terminate near 100 and 58 kJ mol^{-1} resulting in relatively narrow laboratory angular distributions and TOF spectra.

The calculations reveal that the 1-propynyl radical adds with its radical center to the π-electrons of ethylene without an entrance barrier forming the initial adduct **i1**. Intermediate **i1** can eliminate the ethylenic hydrogen atom to form 1-penten-3-yne (**p1**) plus atomic hydrogen via a transition state lying 22 kJ mol^{-1} above the separated products. The computed exit geometries for the departing hydrogen atom in the **i1** → **p1** + H transition state indicates that the hydrogen atom departs at 78.2° with respect to the rotating plane of the decomposing complex (Figure 5)

and agrees with the sideways scattering identified in the *T(θ)* distribution (Figure 3). The potential cyclic product vinylidene-cyclopropane (**p7**) can be formed by methyl hydrogen atom elimination from intermediate **i1** via a transition state through an exit barrier of 14 kJ mol^{-1}. Intermediate **i1** can also isomerize by hydrogen migration from the C_2H_4 moiety to form **i2**. Unimolecular decomposition of **i2** by hydrogen atom elimination from the C_2H_4 group yields **p1** + H. The computed exit geometry for the **i2** → **p1** transition state suggests that the product would be also sideways scattered (Figure 5), where atomic hydrogen is emitted at an angle of 80.6° with respect to the rotational plane of the decomposing complex. Besides dissociation to **p1** + H, intermediate **i2** can produce penta-1,2,3-triene (**p2**) by eliminating a methyl hydrogen atom from the propynyl group. The barrier to cyclization **i1** → **i3** is only 10 kJ mol^{-1} higher than that required for **i1** → **i2** isomerization, where the terminal methylene groups attacks the π electrons at methyl-substituted carbon atom resulting in a 4-membered ring stabilized by 204 kJ mol^{-1} with respect to the reactants. Intermediate **i3** can isomerize by hydrogen migration to **i6** via a high energy transition state, which then eliminates a methyl hydrogen atom to form the methylene cyclobutene **p4** isomer. Lastly, intermediate **i1** can undergo a 1,2-hydrogen migration from its methylene group to the neighboring acetylenic carbon atom to form **i4**, which then dissociates to **p1** + H by ejecting the hydrogen atom in the rotational plane (0°) of the decomposing complex (Figure 5). Intermediate **i4** can instead cyclize to **i6** via a 115 kJ mol^{-1} barrier, or to **i5** via a 176 kJ mol^{-1} barrier by hydrogen migration from the methyl group of resulting in a C5 backbone that can decompose to **p3** by emitting a hydrogen atom. Alternatively, **i5** can *cis-trans* isomerize to **i7** which can dissociate to **p6** + H via a loose transition state 11 kJ mol^{-1} above the product channel. Also, intermediate **i7** may cyclize forming a saturated carbon pentagon **i8** that precedes formation of the thermodynamically favored cyclopentadiene **p5** isomer. Note that the products **p1** and **p5** can interconvert via multiple isomerization steps (Figure 6); but the relative energies of the intermediates (**i9**, **i12 - i17**) and the related transition states are not accessible under our experimental conditions. In brief, **p1** can be formed via three pathways (8), with the hydrogen eliminated from the C_2H_4 group. Products **p2 - p7** can be accessed via pathways ((9)-(14)) by atomic hydrogen elimination from the methyl group, which is located at the propynyl radical reactant.

$$CH_3CC + C_2H_4 \rightarrow \mathbf{[i1]/[\ i1 \rightarrow i2]/[\ i1 \rightarrow i4]} \rightarrow \mathbf{p1} + H \qquad (8)$$

$CH_3CC + C_2H_4 \rightarrow$ **i1** $\rightarrow$ **i2** $\rightarrow$ **p2** + H (9)

$CH_3CC + C_2H_4 \rightarrow$ **i1** $\rightarrow$ **i4** $\rightarrow$ **i5** $\rightarrow$ **p3** + H (10)

$CH_3CC + C_2H_4 \rightarrow$ [**i1** $\rightarrow$ **i3** $\rightarrow$ **i6**]/[**i1** $\rightarrow$ **i4** $\rightarrow$ **i6**] $\rightarrow$ **p4** + H (11)

$CH_3CC + C_2H_4 \rightarrow$ **i1** $\rightarrow$ **i4** $\rightarrow$ **i5** $\rightarrow$ **i7** $\rightarrow$ **i8** $\rightarrow$ **p5** + H (12)

$CH_3CC + C_2H_4 \rightarrow$ **i1** $\rightarrow$ **i4** $\rightarrow$ **i5** $\rightarrow$ **i7** $\rightarrow$ **p6** + H (13)

$CH_3CC + C_2H_4 \rightarrow$ **i1** $\rightarrow$ **p7** + H (14)

In summary, considering the experimentally derived reaction energy of 111 ± 16 kJ mol^{-1} along with the experimental findings of a tight exit transition state from decomposing long lived reaction intermediate(s) and the aforementioned geometrical constraints of the hydrogen atom emission nearly perpendicularly to the rotational plane of the decomposing complex, product **p1** along with atomic hydrogen is likely formed through intermediates **i1** and/or **i2**. However, in principle, the formation of the thermodynamically less stable isomers **p2 - p4** and **p6 - p7** cannot be ruled out since their formation might be masked in the low energy tail of the center-of-mass translational energy distribution. Nevertheless, the results of the aforementioned isotopic substitution experiments reveal that only the atomic deuterium loss channel was observed in the reaction of 1-propynyl with ethylene-d_4. Figure 7 traces the hydrogen versus deuterium loss in the 1-propynyl - ethylene-d_4 system. Here, only one channel is consistent with the experimentally observed atomic deuterium loss, i.e. the formation of 1-penten-3-yne (**p1**); the remaining channels only lead to atomic hydrogen loss from the methyl group of the former 1-propynyl moiety. Therefore, we can conclude that based on the isotopic substitution experiments, 1-penten-3-yne (**p1**) represents the sole C_5H_6 isomer formed under our experimental conditions with the hydrogen atom emitted from the ethylene reactant.

To assess to what extent **p2 - p7** could be formed in this experiment, we calculated the statistical yields of products **p1 - p7** using RRKM theory. The branching ratios are tabulated in Table 2 and predict that – in agreement with our experiments - 1-penten-3-yne (**p1**) constitutes the nearly exclusive product with the fraction exceeding 99 % of the total C_5H_6 yield at E_C = 31.1 kJ mol^{-1}. Dissociation from intermediate **i1** supplies 34.85% and intermediate **i2** contributes 64.85% with the remaining 0.30 % attributed to the **i4** pathway. This finding is consistent with the computed geometries of the exit transition states involved in the formation of 1-penten-3-yne (**p1**) revealing that **p1** can be formed from intermediates **i1** and **i2** (sideways scattering). It is

important to highlight that under single collision conditions, the nascent reaction products fly apart in the unimolecular decomposition of the intermediate(s). Further, accounting for energy and angular momentum conservation along with the findings of the center-of-mass translational energy distribution, a large fraction of **p1** holds significant internal (rovibrational energy). Can this internal energy be utilized to isomerize to the thermodynamically more stable isomer **p5** thus reaching an equilibrium between **p1** and **p5**? In this case, due to the single collision conditions, the center-of-mass translational energy distribution would still be 'locked' revealing the overall formation of **p1**, but the internal energy can be used to isomerize to **p5**. Considering the possible isomerization of **p1** to **p5**, the isomerization of **p1** to **i9** initiates the rearrangement and is inhibited by a transition state located 199 kJ mol^{-1} above the separated reactants. Therefore, at the collision energy of 31.1 kJ mol^{-1}, this pathway is closed.

5. Conclusion

The crossed molecular beam reactions of the 1-propynyl radical (CH_3CC; X^2A_1) with ethylene (H_2CCH_2; X^1A_{1g}) and ethylene-d_4 (D_2CCD_2; X^1A_{1g}) were investigated at collision energies of 31 kJ mol^{-1} to explore the formation of C_5H_6 isomers under single-collision conditions. Our experimental results and the doublet C_5H_7 PES combined show that the 1-propynyl-ethylene reaction is initiated by the barrierless addition of the 1-propynyl radical to the π-electron density of ethylene leading to an acyclic C_5H_7 intermediate. The reaction eventually produces 1-penten-3-yne (**p1**) plus hydrogen atom with an overall reaction exoergicity of 111 ± 16 kJ mol^{-1} thus revealing that the methyl group in the 1-propynyl radical acts as a spectator. About 35% of **p1** originates from the initial collision complex followed by C–H bond rupture via a tight exit transition state located 22 kJ mol^{-1} above the separated products. The collision complex (**i1**) can also undergo a [1,2] hydrogen atom shift to the $CH_3CHCCCH_3$ intermediate (**i2**) prior to a hydrogen atom release; RRKM calculations suggest that this pathway contributes to about 65% of **p1**.

The C_5H_6 isomers produced in 1-propynyl reactions with ethylene might eventually lead to the resonance-stabilized cyclopentadienyl radical (c-C_5H_5) which is known to participate in PAH growth in combustion-like settings. The low-energy cyclopentadiene isomer **p5** could easily form c-C_5H_5 through loss of a methylene hydrogen atom,[116] but the path from **p1** to **p5** is inhibited by a rather large barrier of 311 kJ mol^{-1} (Figure 6). Instead, more competitive routes are

found through thermal degradation and/or H abstraction reactions leading to the loss of a methyl hydrogen atom from **p1** resulting in acyclic C_5H_5 isomers that, via a series of relatively low energy isomerization steps facilitating ring closure and ultimately resonance stabilization, lead to the cyclopentadienyl radical.[117]

The isolobal reactions of the ethynyl radical (C_2H) with ethylene-d_4 and of the cyano (CN) radical with ethylene were also initiated by the barrierless addition of the doublet radical reactant to the π-electron density of the unsaturated ethylene.[118-120] The reaction intermediates decompose via tight exit transition states, leading to vinylacetylene ($HCCC_2H_3$) plus a hydrogen atom - while conserving the ethynyl group - and vinylcyanide (C_2H_3CN) along with a hydrogen atom, respectively. Likewise, an analogous reaction mechanisms was found for the reactions of the boron monoxide radical (^{11}BO) with ethylene[121] and between boron sulfide ($^{11}B^{32}S$) with ethylene.[122] Here, the doublet radical boron monoxide (^{11}BO) / boron sulfide ($^{11}B^{32}S$) attacks ethylene with the radical center located at the boron atom and adds to one carbon atom of ethylene. The initial collision complex either decomposes to the vinyl boron monoxide ($C_2H_3{}^{11}BO$) / vinylsulfidoboron molecule ($C_2H_3{}^{11}B^{32}S$) plus a hydrogen atom via a tight exit transition state or undergoes a [1,2] H atom shift to form $CH_3CH^{11}BO$/ $CH_3CH^{11}B^{32}S$ followed by a hydrogen loss. Both processes lead to the same product – the vinyl boron monoxide ($C_2H_3{}^{11}BO$) / vinylsulfidoboron molecule ($C_2H_3{}^{11}B^{32}S$). The preferred sideways scattering combined with RRKM calculations indicate that the dominant channel for the final product is the isomerization process involving hydrogen migration and decomposition thus providing an overall global picture of the reactivity of small doublet radicals with ethylene through eventually barrierless addition – hydrogen atom elimination involving a radical substitution pathway.

Supplementary information

See Supplementary Information for optimized Cartesian coordinates and vibrational frequencies for all intermediates, transition states, reactants and products involved in the reactions of the propynyl radical with ethylene.

Conflicts of interest

There are no conflicts to declare.

Acknowledgements

This work was supported by the U.S. Department of Energy, Basic Energy Sciences DE-FG02-03ER15411 and DE-FG02-04ER15570 to the University of Hawaii and to Florida International University, respectively. Theoretical calculations at Samara University were supported by the Russian Ministry of Science and Higher Education within the major project "Reaction Kinetics and Dynamics in Combustion, Astrochemistry and Astrobiology" on fundamental research in priority areas outlined by the Presidium of the Russian Academy of Sciences.

References

1. H. Richter and J. B. Howard, *Prog. Energy Combust. Sci.*, 2000, **26**, 565-608.
2. W. W. Duley, *Faraday Discuss.*, 2006, **133**, 415-425.
3. M. Frenklach and E. D. Feigelson, *Astrophys. J.*, 1989, **341**, 372-384.
4. A. G. G. M. Tielens, *Annu. Rev. Astron. Astr.*, 2008, **46**, 289-337.
5. N. A. Eaves, S. B. Dworkin and M. J. Thomson, *Proc. Combust. Inst.*, 2017, **36**, 935-945.
6. Z. A. Mansurov, *Combust. Explo. Shock+*, 2005, **41**, 727-744.
7. K. H. Kim, S. A. Jahan, E. Kabir and R. J. C. Brown, *Environ. Int.*, 2013, **60**, 71-80.
8. D. Majumdar, B. Rajaram, S. Meshram and C. V. Chalapati Rao, *Crit. Rev. Env. Sci. Technol.*, 2012, **42**, 1191-1232.
9. B. M. Jones, F. Zhang, R. I. Kaiser, A. Jamal, A. M. Mebel, M. A. Cordiner and S. B. Charnley, *Proc. Nat. Acad. Sci. U.S.A.*, 2011, **108**, 452-457.
10. N. Balucani, O. Asvany, Y. Osamura, L. C. L. Huang, Y. T. Lee and R. I. Kaiser, *Planet. Space Sci.*, 2000, **48**, 447-462.
11. N. Balucani, O. Asvany, R. I. Kaiser and Y. Osamura, *J. Phys. Chem. A*, 2002, **106**, 4301-4311.
12. L. C. L. Huang, N. Balucani, Y. T. Lee, R. I. Kaiser and Y. Osamura, *J. Chem. Phys.*, 1999, **111**, 2857-2860.
13. H. Naraoka, A. Shimoyama and K. Harada, *Earth Planet. Sci. Lett.*, 2000, **184**, 1-7.
14. L. Becker and T. E. Bunch, *Meteorit. Planet. Sci.*, 1997, **32**, 479-487.
15. M. P. Callahan, A. Abo-Riziq, B. Crews, L. Grace and M. S. de Vries, *Spectrochim. Acta, Part A*, 2008, **71**, 1492-1495.
16. L. D'Hendecourt and P. Ehrenfreund, *Adv. Space Res.*, 1997, **19**, 1023-1032.
17. E. F. Van Dishoeck, *Publ. Astron. Soc. Pac.*, 2000, **112**, 286-287.
18. Y. M. Rhee, T. J. Lee, M. S. Gudipati, L. J. Allamandola and M. Head-Gordon, *Proc. Nat. Acad. Sci. U.S.A.*, 2007, **104**, 5274-5278.
19. L. J. Allamandola, A. G. G. M. Tielens and J. R. Barker, *Astrophys. J. Suppl. S.*, 1989, **71**, 733-775.
20. M. Steglich, J. Bouwman, F. Huisken and T. Henning, *Astrophys. J.*, 2011, **742**, 2.
21. M. Steglich, C. Jäger, G. Rouillé, F. Huisken, H. Mutschke and T. Henning, *Astrophys. J. Lett.*, 2010, **712**, L16.
22. A. M. Ricks, G. E. Douberly and M. A. Duncan, *Astrophys. J.*, 2009, **702**, 301.
23. J. L. Puget and A. Léger, *Annu. Rev. Astron. Astr.*, 1989, **27**, 161-198.
24. P. Schmitt-Kopplin, Z. Gabelica, R. D. Gougeon, A. Fekete, B. Kanawati, M. Harir, I. Gebefuegi, G. Eckel and N. Hertkorn, *Proc. Nat. Acad. Sci. U.S.A.*, 2010, **107**, 2763-2768.
25. L. M. Ziurys, *Proc. Nat. Acad. Sci. U.S.A.*, 2006, **103**, 12274-12279.
26. M. P. Bernstein, S. A. Sandford, L. J. Allamandola, J. S. Gillette, S. J. Clemett and R. N. Zare, *Science*, 1999, **283**, 1135-1138.
27. P. Ehrenfreund and M. A. Sephton, *Faraday Discuss.*, 2006, **133**, 277-288.
28. E. Herbst and E. F. Van Dishoeck, *Annu. Rev. Astron. Astr.*, 2009, **47**, 427-480.
29. A. M. Mebel, V. V. Kislov and R. I. Kaiser, *J. Am. Chem. Soc.*, 2008, **130**, 13618-13629.
30. S. Messenger, S. Amari, X. Gao, R. M. Walker, S. J. Clemett, X. D. F. Chillier, R. N. Zare and R. S. Lewis, *Astrophys. J.*, 1998, **502**, 284-295.

31. S. Mostefaoui, P. Hoppe and A. El Goresy, *Science*, 1998, **280**, 1418-1420.
32. P. P. K. Smith and P. R. Buseck, *Geochim. Cosmochim. Acta Suppl.*, 1982, **16**, 1167-1175.
33. W. W. Duley, *Astrophys. J.*, 2000, **528**, 841-848.
34. S. Amari, R. S. Lewis and E. Anders, *Geochim. Cosmochim. Acta*, 1995, **59**, 1411-1426.
35. E. Zinner, S. Amari, B. Wopenka and R. S. Lewis, *Meteoritics*, 1995, **30**, 209-226.
36. J. Cami, J. Bernard-Salas, E. Peeters and S. E. Malek, *Science*, 2010, **329**, 1180-1182.
37. A. L. Lafleur, J. B. Howard, J. A. Marr and T. Yadav, *J. Phys. Chem.*, 1993, **97**, 13539-13543.
38. N. S. Goroff, *Acc. Chem. Res.*, 1996, **29**, 77-83.
39. A. L. Lafleur, J. B. Howard, K. Taghizadeh, E. F. Plummer, L. T. Scott, A. Necula and K. C. Swallow, *J. Phys. Chem.*, 1996, **100**, 17421-17428.
40. L. Vereecken, J. Peeters, H. F. Bettinger, R. I. Kaiser, P. V. R. Schleyer and H. F. Schaefer, *J. Am. Chem. Soc.*, 2002, **124**, 2781-2789.
41. R. I. Kaiser, D. Stranges, H. M. Bevsek, Y. T. Lee and A. G. Suits, *J. Chem. Phys.*, 1997, **106**, 4945-4953.
42. R. I. Kaiser, Y. T. Lee and A. G. Suits, *J. Chem. Phys.*, 1995, **103**, 10395-10398.
43. R. I. Kaiser, N. Balucani, D. O. Charkin and A. M. Mebel, *Chem. Phys. Lett.*, 2003, **382**, 112-119.
44. F. Stahl, P. V. R. Schleyer, H. F. Schaefer III and R. I. Kaiser, *Planet. Space Sci.*, 2002, **50**, 685-692.
45. T. L. Nguyen, A. M. Mebel and R. I. Kaiser, *J. Phys. Chem. A*, 2001, **105**, 3284-3299.
46. R. I. Kaiser, I. Hahndorf, L. C. L. Huang, Y. T. Lee, H. F. Bettinger, P. V. R. Schleyer, H. F. Schaefer III and P. R. Schreiner, *J. Chem. Phys.*, 1999, **110**, 6091-6094.
47. R. I. Kaiser, D. Stranges, Y. T. Lee and A. G. Suits, *Astrophys. J.*, 1997, **477**, 982.
48. N. Balucani, A. M. Mebel, Y. T. Lee and R. I. Kaiser, *J. Phys. Chem. A*, 2001, **105**, 9813-9818.
49. R. I. Kaiser, A. M. Mebel, A. H. H. Chang, S. H. Lin and Y. T. Lee, *J. Chem. Phys.*, 1999, **110**, 10330-10344.
50. F. Stahl, P. V. R. Schleyer, H. F. Bettinger, R. I. Kaiser, Y. T. Lee and H. F. Schaefer III, *J. Chem. Phys.*, 2001, **114**, 3476-3487.
51. R. I. Kaiser, A. M. Mebel and Y. T. Lee, *J. Chem. Phys.*, 2001, **114**, 231-239.
52. M. Frenklach and H. Wang, *Proc. Combust. Inst.*, 1991, **23**, 1559-1566.
53. D. S. N. Parker, R. I. Kaiser, T. P. Troy and M. Ahmed, *Angew. Chem. Int. Ed.*, 2014, **53**, 7740-7744.
54. D. S. N. Parker, R. I. Kaiser, B. Bandyopadhyay, O. Kostko, T. P. Troy and M. Ahmed, *Angew. Chem. Int. Ed.*, 2015, **54**, 5421-5424.
55. T. Yang, R. I. Kaiser, T. P. Troy, B. Xu, O. Kostko, M. Ahmed, A. M. Mebel, M. V. Zagidullin and V. N. Azyazov, *Angew. Chem. Int. Ed.*, 2017, **129**, 4586-4590.
56. A. M. Mebel, Y. Georgievskii, A. W. Jasper and S. J. Klippenstein, *Proc. Combust. Inst.*, 2017, **36**, 919-926.
57. J. D. Bittner and J. B. Howard, *Proc. Combust. Inst.*, 1981, **18**, 1105-1116.
58. J. Appel, H. Bockhorn and M. Frenklach, *Combust. Flame*, 2000, **121**, 122-136.
59. A. M. Mebel, A. Landera and R. I. Kaiser, *J. Phys. Chem. A*, 2017, **121**, 901-926.
60. L. Zhao, R. I. Kaiser, B. Xu, U. Ablikim, M. Ahmed, D. Joshi, G. Veber, F. R. Fischer and A. M. Mebel, *Nature Astronomy*, 2018, **2**, 413-419.

61. D. S. N. Parker, F. Zhang, Y. S. Kim, R. I. Kaiser, A. Landera, V. V. Kislov, A. M. Mebel and A. G. G. M. Tielens, *Proc. Nat. Acad. Sci. U.S.A.*, 2012, **109**, 53-58.
62. R. I. Kaiser, D. S. N. Parker and A. M. Mebel, *Annu. Rev. Phys. Chem.*, 2015, **66**, 43-67.
63. L. Zhao, R. I. Kaiser, B. Xu, U. Ablikim, M. Ahmed, M. M. Evseev, E. K. Bashkirov, V. N. Azyazov and A. M. Mebel, *Nature Astronomy*, 2018, **2**, 973.
64. C. H. Chin, W. K. Chen, W. J. Huang, Y. C. Lin and S. H. Lee, *Icarus*, 2013, **222**, 254-262.
65. A. Coustenis, A. Salama, B. Schulz, S. Ott, E. Lellouch, T. H. Encrenaz, D. Gautier and H. Feuchtgruber, *Icarus*, 2003, **161**, 383-403.
66. L. Zhao, R. I. Kaiser, B. Xu, U. Ablikim, M. Ahmed, M. V. Zagidullin, V. N. Azyazov, A. H. Howlader, S. F. Wnuk and A. M. Mebel, *J. Phys. Chem. Lett.*, 2018, **9**, 2620-2626.
67. L. Zhao, B. Xu, U. Ablikim, W. Lu, M. Ahmed, M. M. Evseev, E. K. Bashkirov, V. N. Azyazov, A. H. Howlader, S. F. Wnuk, A. M. Mebel and R. I. Kaiser, *ChemPhysChem*, 2019, **20**, 791-797.
68. A. Raj, I. D. C. Prada, A. A. Amer and S. H. Chung, *Combust. Flame*, 2012, **159**, 500-515.
69. S. Park, Y. Wang, S. H. Chung and S. M. Sarathy, *Combust. Flame*, 2017, **178**, 46-60.
70. N. M. Marinov, W. J. Pitz, C. K. Westbrook, A. M. Vincitore, M. J. Castaldi, S. M. Senkan and C. F. Melius, *Combust. Flame*, 1998, **114**, 192-213.
71. N. M. Marinov, W. J. Pitz, C. K. Westbrook, M. J. Castaldi and S. M. Senkan, *Combust. Sci. Technol.*, 1996, **116**, 211-287.
72. N. M. Marinov, M. J. Castaldi, C. F. Melius and W. Tsang, *Combust. Sci. Technol.*, 1997, **128**, 295-342.
73. C. F. Melius, M. E. Colvin, N. M. Marinov, W. J. Pit and S. M. Senkan, *Symp. (Int.) Combust.*, 1996, **26**, 685-692.
74. V. V. Kislov and A. M. Mebel, *J. Phys. Chem. A*, 2008, **112**, 700-716.
75. N. Hansen, S. J. Klippenstein, J. A. Miller, J. Wang, T. A. Cool, M. E. Law, P. R. Westmoreland, T. Kasper and K. Kohse-Höinghaus, *J. Phys. Chem. A*, 2006, **110**, 4376-4388.
76. http://www.astrochymist.org.
77. C. M. Gong, H. B. Ning, Z. R. Li and X. Y. Li, *Theor. Chem. Acc.*, 2015, **134**, 1599.
78. I. Hahndorf, H. Y. Lee, A. M. Mebel, S. H. Lin, Y. T. Lee and R. I. Kaiser, *J. Chem. Phys.*, 2000, **113**, 9622-9636.
79. L. C. L. Huang, H. Y. Lee, A. M. Mebel, S. H. Lin, Y. T. Lee and R. I. Kaiser, *J. Chem. Phys.*, 2000, **113**, 9637-9648.
80. N. Balucani, H. Y. Lee, A. M. Mebel, Y. T. Lee and R. I. Kaiser, *J. Chem. Phys.*, 2001, **115**, 5107-5116.
81. B. B. Dangi, S. Maity, R. I. Kaiser and A. M. Mebel, *J. Phys. Chem. A*, 2013, **117**, 11783-11793.
82. B. Yang, P. Oßwald, Y. Li, J. Wang, L. Wei, Z. Tian, F. Qi and K. Kohse-Höinghaus, *Combust. Flame*, 2007, **148**, 198-209.
83. T. Zhang, J. Wang, T. Yuan, X. Hong, L. Zhang and F. Qi, *J. Phys. Chem. A*, 2008, **112**, 10487-10494.
84. N. Hansen, S. J. Klippenstein, C. A. Taatjes, J. A. Miller, J. Wang, T. A. Cool, B. Yang, R. Yang, L. Wei, C. Huang, J. Wang, F. Qi, M. E. Law and P. R. Westmoreland, *J. Phys. Chem. A*, 2006, **110**, 3670-3678.

85. A. M. Mebel and V. V. Kislov, *J. Phys. Chem. A*, 2009, **113**, 9825-9833.
86. V. V. Kislov and A. M. Mebel, *J. Phys. Chem. A*, 2007, **111**, 9532-9543.
87. D. H. Kim, J. A. Mulholland, D. Wang and A. Violi, *J. Phys. Chem. A*, 2010, **114**, 12411-12416.
88. D. Wang, A. Violi, D. H. Kim and J. A. Mullholland, *J. Phys. Chem. A*, 2006, **110**, 4719-4725.
89. M. R. Djokic, K. M. Van Geem, C. Cavallotti, A. Frassoldati, E. Ranzi and G. B. Marin, *Combust. Flame*, 2014, **161**, 2739-2751.
90. R. I. Kaiser, P. Maksyutenko, C. Ennis, F. Zhang, X. Gu, S. P. Krishtal, A. M. Mebel, O. Kostko and M. Ahmed, *Faraday Discuss.*, 2010, **147**, 429-478.
91. A. M. Thomas, L. Zhao, C. He, A. M. Mebel and R. I. Kaiser, *J. Phys. Chem. A*, 2018, **122**, 6663-6672.
92. G. O. Brink, *Rev. Sci. Instrum.*, 1966, **37**, 857-860.
93. N. R. Daly, *Rev. Sci. Instrum.*, 1960, **31**, 264-267.
94. M. F. Vernon, *Molecular Beam Scattering*, Ph. D. thesis, University of California at Berkeley, Berkeley, CA, 1983.
95. P. S. Weiss, *Reaction Dynamics of Electronically Excited Alkali Atoms with Simple Molecules*, Ph. D. thesis, University of California at Berkeley, Berkeley, CA, 1986.
96. M. Saeys, M. F. Reyniers, G. B. Marin, V. Van Speybroeck and M. Waroquier, *AlChE J.*, 2004, **50**, 426-444.
97. M. Saeys, M. F. Reyniers, G. B. Marin, V. Van Speybroeck and M. Waroquier, *J. Phys. Chem. A*, 2003, **107**, 9147-9159.
98. A. D. Becke, *J. Chem. Phys.*, 1993, **98**, 5648-5652.
99. C. Lee, W. Yang and R. G. Parr, *Phys. Rev. B: Condens. Matter*, 1988, **37**, 785.
100. T. B. Adler, G. Knizia and H. J. Werner, *J. Chem. Phys.*, 2007, **127**, 221106.
101. G. Knizia, T. B. Adler and H. J. Werner, *J. Chem. Phys.*, 2009, **130**, 054104.
102. T. H. Dunning Jr, *J. Chem. Phys.*, 1989, **90**, 1007-1023.
103. H. J. Werner, P. J. Knowles, R. Lindh, F. R. Manby, M. Schütz, P. Celani, T. Korona, G. Rauhut, R. D. Amos and A. Bernhardsson, *MOLPRO, Version 2010.1, A Package of Ab Initio Programs*, University of Cardiff: Cardiff, UK, see http://www.molpro.net, 2010.
104. J. Zhang and E. F. Valeev, *J. Chem. Theory Comput.*, 2012, **8**, 3175-3186.
105. M. J. Frisch, G. W. Trucks, H. B. Schlegel, G. E. Scuseria, M. A. Robb, J. R. Cheeseman, G. Scalmani, V. Barone, B. Mennucci and G. A. Petersson, Gaussian 09 Revision A. 1, Gaussian, Inc., Wallingford CT, USA, 2009.
106. P. J. Robinson and K. A. Holbrook, *Unimolecular Reactions*, John Wiley & Sons, Ltd.: New York, NY, 1972.
107. H. Eyring, S. H. Lin and S. M. Lin, *Basic Chemical Kinetics*, John Wiley & Sons, Ltd.: New York, NY, 1980.
108. J. I. Steinfeld, J. S. Francisco and W. L. Hase, *Chemical Kinetics and Dynamics*, Prentice Hall: Englewood Cliffs (New Jersey), 1982.
109. C. He, L. Zhao, A. M. Thomas, A. N. Morozov, A. M. Mebel and R. I. Kaiser, *J. Phys. Chem. A*, 2019, **123**, 5446-5462.
110. V. V. Kislov, T. L. Nguyen, A. M. Mebel, S. H. Lin and S. C. Smith, *J. Chem. Phys.*, 2004, **120**, 7008-7017.
111. R. D. Levine, *Molecular Reaction Dynamics*, Cambridge University Press, 2005.

112. R. I. Kaiser, C. C. Chiong, O. Asvany, Y. T. Lee, F. Stahl, P. Von R. Schleyer and H. F. Schaefer III, *J. Chem. Phys.*, 2001, **114**, 3488-3496.
113. N. Balucani, O. Asvany, A. H. H. Chang, S. H. Lin, Y. T. Lee, R. I. Kaiser, H. F. Bettinger, P. V. R. Schleyer and H. F. Schaefer III, *J. Chem. Phys.*, 1999, **111**, 7472-7479.
114. X. Gu and R. I. Kaiser, *Acc. Chem. Res.*, 2008, **42**, 290-302.
115. W. B. Miller, S. A. Safron and D. R. Herschbach, *Discuss. Faraday Soc.*, 1967, **44**, 108-122.
116. C. Cavallotti, D. Polino, A. Frassoldati and E. Ranzi, *J. Phys. Chem. A*, 2012, **116**, 3313-3324.
117. J. D. Savee, T. M. Selby, O. Welz, C. A. Taatjes and D. L. Osborn, *J. Phys. Chem. Lett.*, 2015, **6**, 4153-4158.
118. F. Zhang, Y. S. Kim, R. I. Kaiser, S. P. Krishtal and A. M. Mebel, *J. Phys. Chem. A*, 2009, **113**, 11167-11173.
119. N. Balucani, O. Asvany, A. H. H. Chang, S. H. Lin, Y. T. Lee, R. I. Kaiser and Y. Osamura, *J. Chem. Phys.*, 2000, **113**, 8643-8655.
120. D. S. N. Parker, A. M. Mebel and R. I. Kaiser, *Chem. Soc. Rev.*, 2014, **43**, 2701-2713.
121. D. S. N. Parker, F. Zhang, P. Maksyutenko, R. I. Kaiser, S. H. Chen and A. H. H. Chang, *Phys. Chem. Chem. Phys.*, 2012, **14**, 11099-11106.
122. T. Yang, B. B. Dangi, D. S. N. Parker, R. I. Kaiser, Y. An and A. H. H. Chang, *Phys. Chem. Chem. Phys.*, 2014, **16**, 17580-17587.
123. https://webbook.nist.gov/chemistry/.

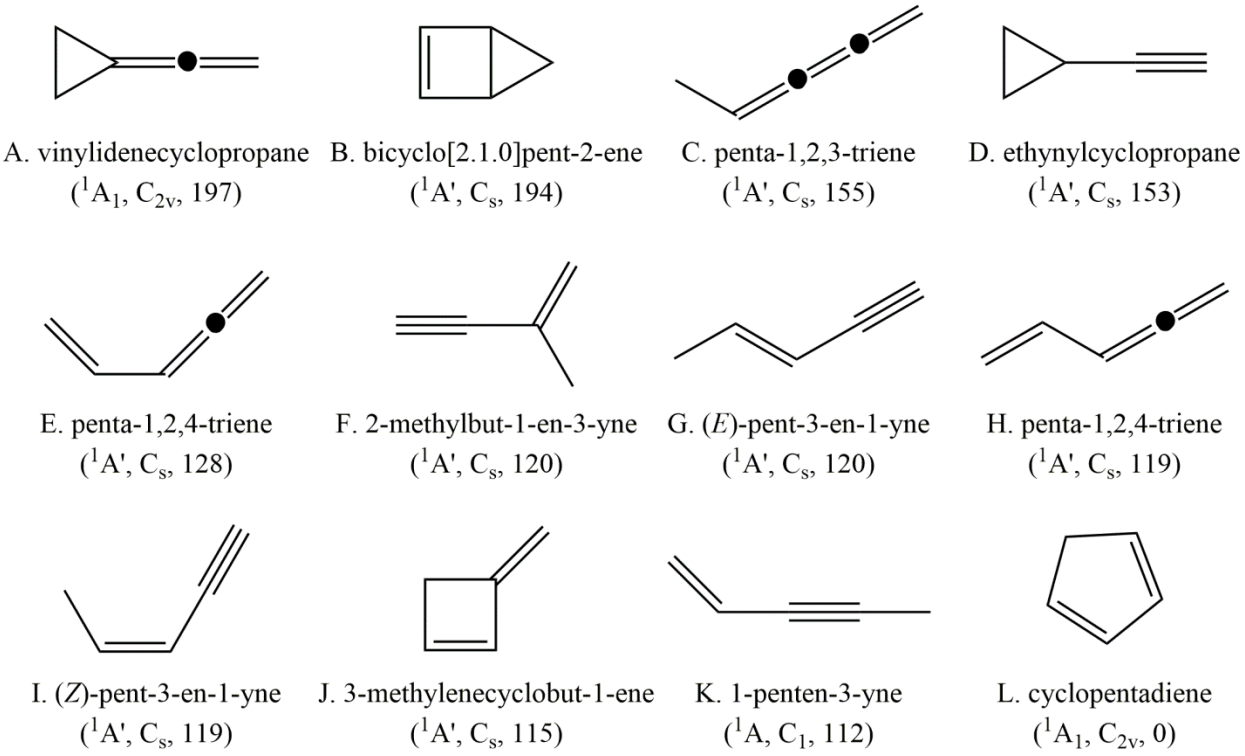

Scheme 1. Structures of selected C_5H_6 isomers along with their point groups and energies (kJ mol^{-1}) relative to cyclopentadiene. The energies were obtained from NIST.[123]

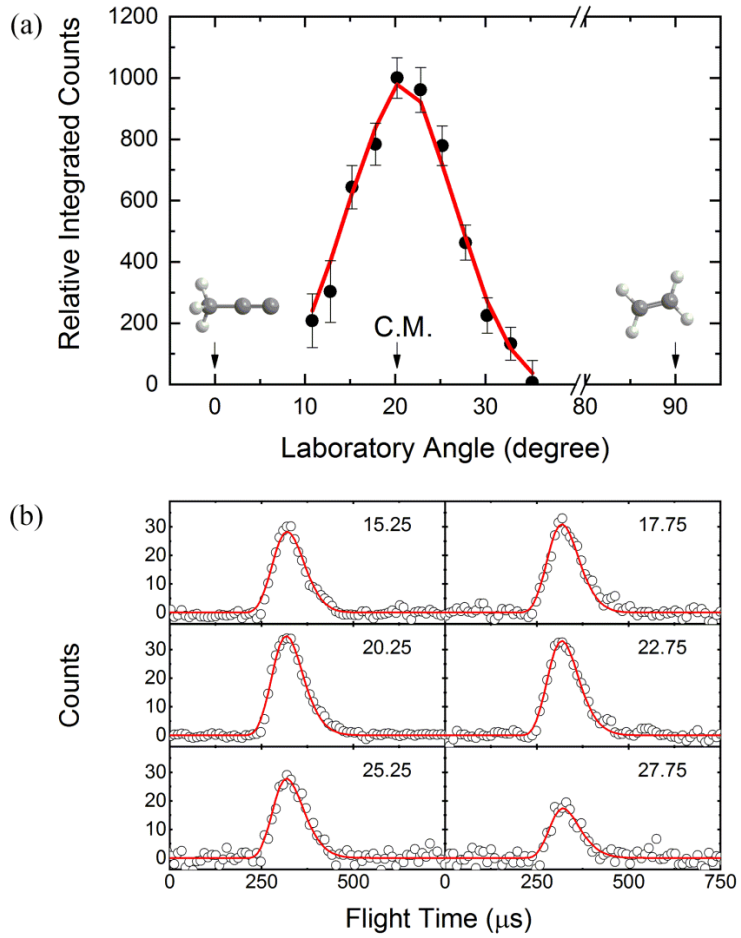

Figure 1. Laboratory angular distribution (top) and time-of-flight (TOF) spectra (bottom) recorded at a mass-to-charge (m/z) of 66 for the reaction of the 1-propynyl radical (CH_3CC; C_{3v}; X^2A_1) with ethylene (C_2H_4; D_{2h}; X^1A_{1g}). The direction of the 1-propynyl radical beam is defined as 0°, that of the ethylene beam as 90°. The solid line represents the best-fit center-of-mass functions depicted in Figure 2. The black circles the experimental data. The open circles represent the experiment TOF spectra. The solid line represents the best fits obtained from the center-of-mass functions.

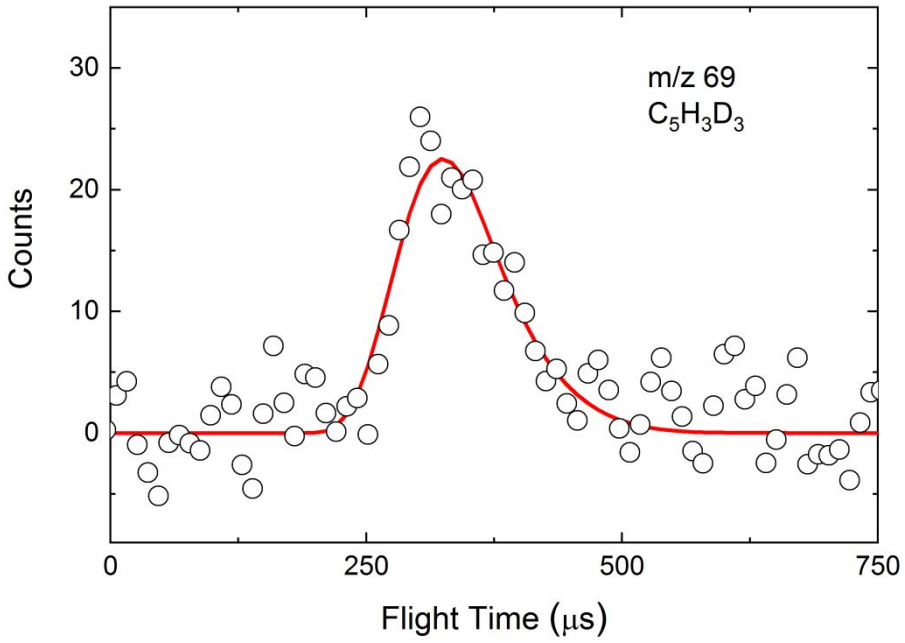

Figure 2. Time-of-flight (TOF) spectra for the reaction of the 1-propynyl radical (CH_3CC; C_{3v}; X^2A_1) with ethylene-d_4 (C_2D_4; D_{2h}; X^1A_{1g}), leading to the D-loss product $C_5H_3D_3$. The open circles represent the experimental data, and the red line represents the fit obtained from the forward-convolution routine.

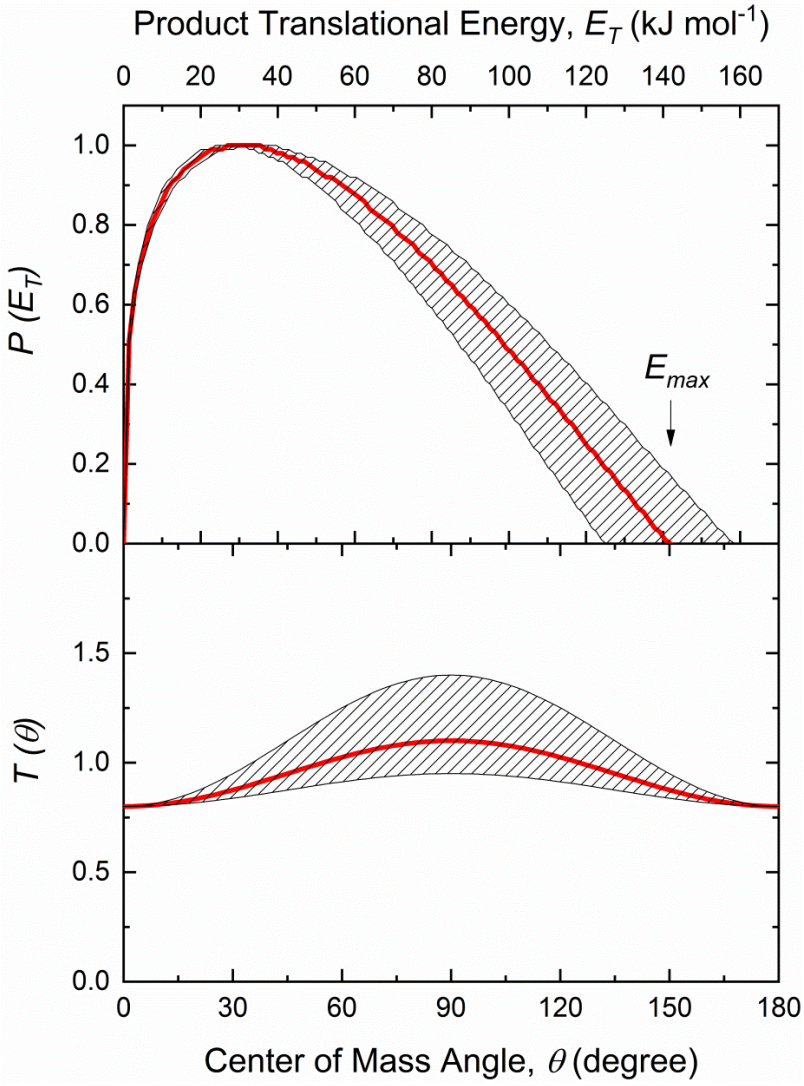

Figure 3. Best-fit center-of-mass angular ($T(\theta)$, lower) and translational energy ($P(E_T)$, upper) flux distributions of the reaction of the 1-propynyl radical with ethylene to form the 1-penten-3-yne molecule plus atomic hydrogen. The red lines are the best fits; the shaded areas delimit the acceptable upper and lower error limits. E_{max} defines the maximum translational energy.

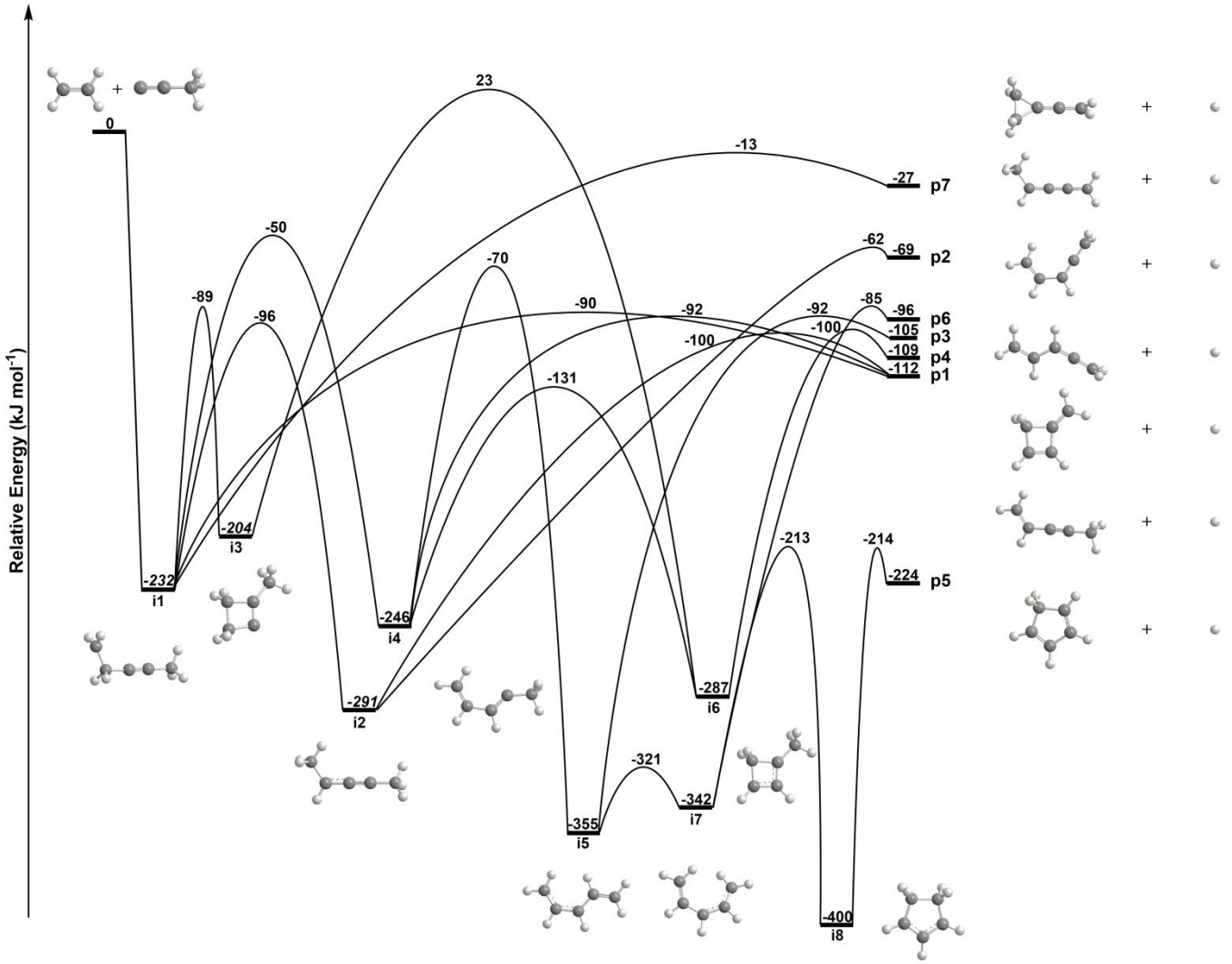

Figure 4. Schematic representation of the potential energy surface of the reaction of the 1-propynyl radical with ethylene. Energies calculated at the CCSD(T)-F12/cc-pVTZ-f12//B3LYP/6-311G(d,p) + ZPE(B3LYP/6-311G(d,p) level are shown in kJ mol^{-1} relative to the energy of the separated reactants. The geometries of the transition states, reactants, intermediates, and products and their point groups and the symmetries of their electronic wave functions are compiled in the Supplementary Information.

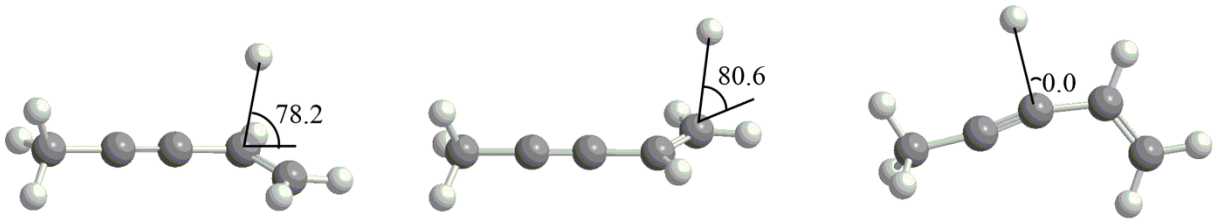

ts i1-p1 ts i2-p1 ts i4-p1

C_1, ^2A C_1, ^2A C_s, $^2A'$

Figure 5. Computed geometries of the exit transition states involved in the formation of 1-penten-3-yne molecule (**p1)**. The angle of the departing hydrogen atom is shown in degrees with respect to the total angular momentum vector of the system.

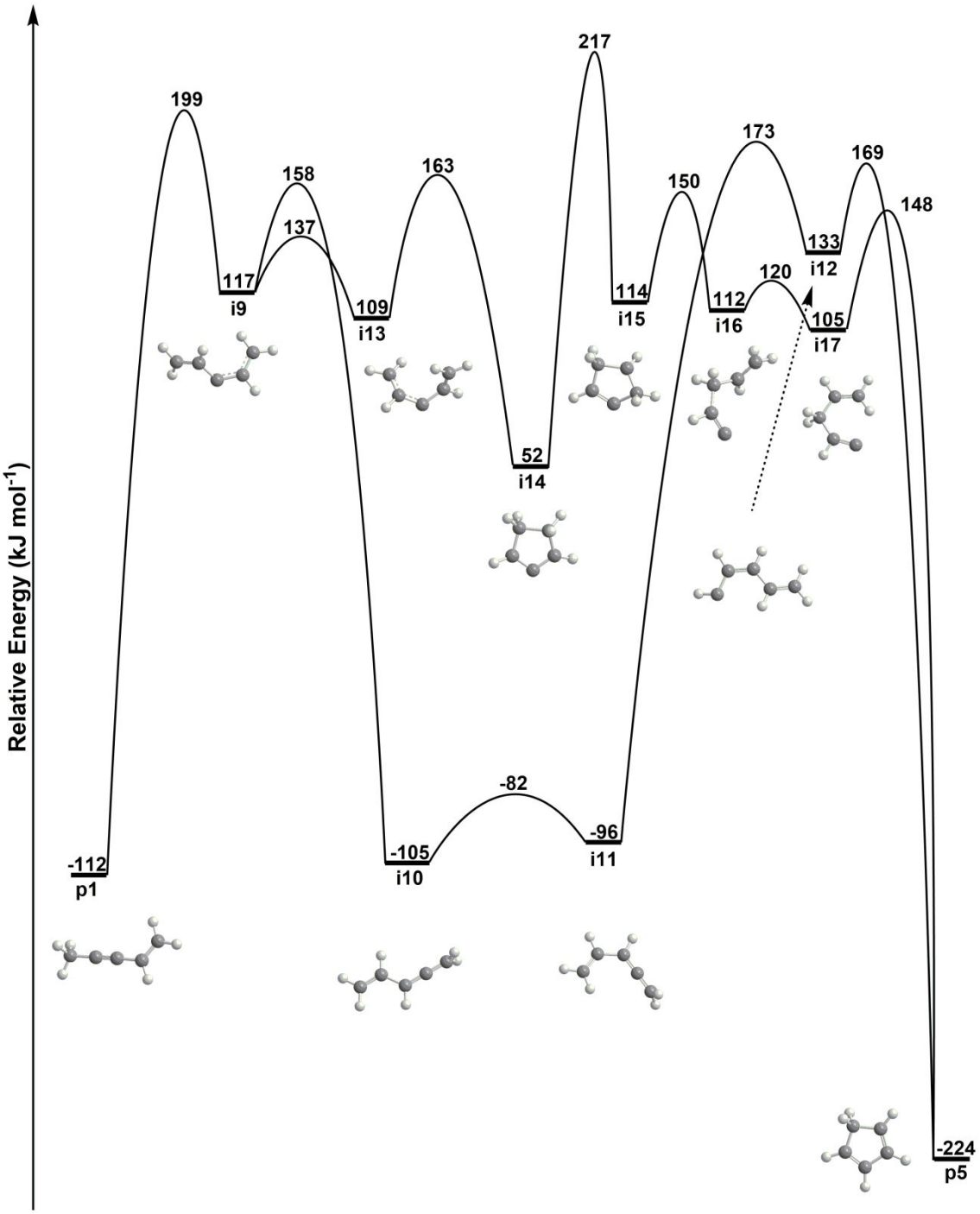

Figure 6. Schematic representation of the potential energy surface for the isomerization of 1-penten-3-yne (**p1)** and cyclopentadiene (**p5)**. Energies calculated at the CCSD(T)-F12/cc-pVTZ-f12//B3LYP/6-311G(d,p) + ZPE(B3LYP/6-311G(d,p) level are shown in kJ mol^{-1} relative to the energy of the separated 1-propynyl and ethylene reactants.

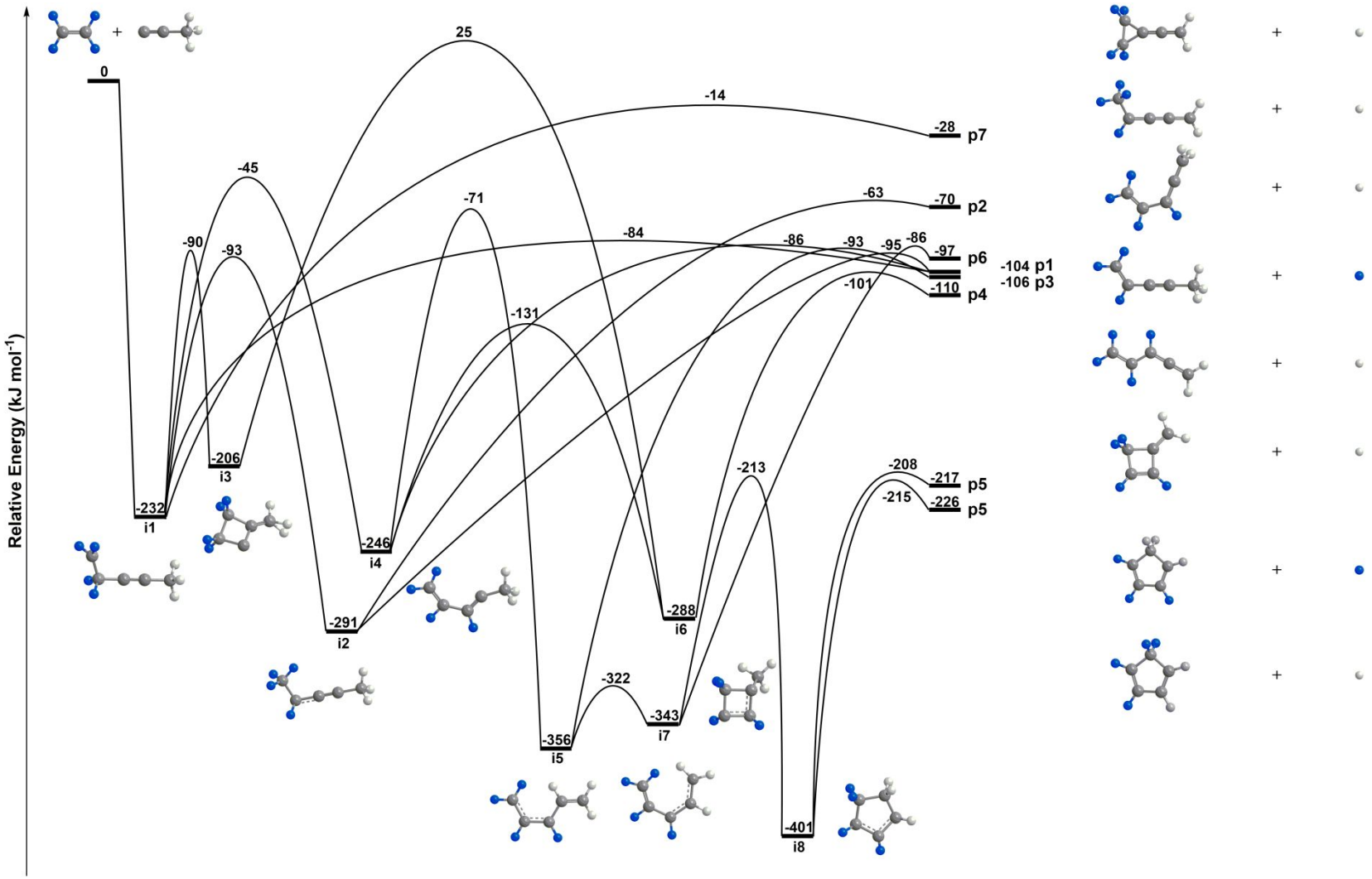

Figure 7. Schematic representation of the potential energy surface of the reaction of the 1-propynyl radical with ethylene-d_4. D atoms from ethylene-d_4 are highlighted in blue.

Table 1. Peak velocities (v_p) and speed ratios (S) of the 1-propynyl (C_3H_3), ethylene (C_2H_4), ethylene-d_4 (C_2D_4) beams along with the corresponding collision energies (E_C) and center-of-mass angles (Θ_{CM}) for each reactive scattering experiment.

Beam	v_p (m s^{-1})	S	E_C (kJ mol^{-1})	Θ_{CM} (degree)
C_3H_3 (X^2A_1)	1740 ± 8	8.1 ± 0.3		
C_2H_4 (X^1A_{1g})	890 ± 15	15.7 ± 0.2	31.1 ± 0.4	20.3 ± 0.3
C_2D_4 (X^1A_{1g})	880 ± 15	15.7 ± 0.2	33.4 ± 0.4	22.8 ± 0.3

Table 2. Statistical branching ratios for the reaction of the 1-propynyl (CH_3CC) radical with ethylene (H_2CCH_2). Here, **p1**-**p7** are 1-penten-3-yne, penta-1,2,3-triene, penta-1,2,4-triene, 3-methylenecyclobut-1-ene, cyclopentadiene, penta-1,2,4-triene and vinylidenecyclopropane.

E_C (kJ mol^{-1})	**p1**	**p2**	**p3**	**p4**	**p5**	**p6**	**p7**
31.1	99.3%	0.70%	0	0	0	0	0

p1	from **i1**	from **i2**	from **i4**
99.3%	34.6%	64.4%	0.30%
100%	34.85%	64.85%	0.30%

Center-of-mass velocity flux contour maps for the reactions of 1-propynyl with ethylene for the atomic hydrogen loss leading to 1-penten-3-yne.